

First Lattice Calculation of the QED Corrections to Leptonic Decay Rates

D. Giusti, V. Lubicz, and C. Tarantino

*Dipartimento di Matematica e Fisica, Università Roma Tre and INFN Sezione di Roma Tre,
Via della Vasca Navale 84, I-00146 Rome, Italy*

G. Martinelli

Dipartimento di Fisica, Università di Roma La Sapienza and INFN Sezione di Roma, Piazzale Aldo Moro 5, 00185 Roma, Italy

C. T. Sachrajda

Department of Physics and Astronomy, University of Southampton, Southampton SO17 1BJ, United Kingdom

F. Sanfilippo and S. Simula

Istituto Nazionale di Fisica Nucleare, Sezione di Roma Tre, Via della Vasca Navale 84, I-00146 Rome, Italy

N. Tantalo

*Dipartimento di Fisica, Università di Roma "Tor Vergata" and INFN Sezione di Tor Vergata,
Via della Ricerca Scientifica 1, I-00133 Roma, Italy*



(Received 27 December 2017; published 13 February 2018)

The leading-order electromagnetic and strong isospin-breaking corrections to the ratio of $K_{\mu 2}$ and $\pi_{\mu 2}$ decay rates are evaluated for the first time on the lattice, following a method recently proposed. The lattice results are obtained using the gauge ensembles produced by the European Twisted Mass Collaboration with $N_f = 2 + 1 + 1$ dynamical quarks. Systematic effects are evaluated and the impact of the quenched QED approximation is estimated. Our result for the correction to the tree-level $K_{\mu 2}/\pi_{\mu 2}$ decay ratio is $-1.22(16)\%$, to be compared to the estimate of $-1.12(21)\%$ based on chiral perturbation theory and adopted by the Particle Data Group.

DOI: [10.1103/PhysRevLett.120.072001](https://doi.org/10.1103/PhysRevLett.120.072001)

Introduction.—The determination of a number of hadronic quantities relevant for flavor physics phenomenology using lattice QCD simulations has reached such an impressive level of precision [1] that both electromagnetic (e.m.) and strong isospin-breaking (IB) effects cannot be neglected.

In the past few years accurate lattice results including e.m. and IB effects have been obtained for the hadron spectrum, as in the case of the charged-neutral mass splittings of pseudoscalar (P) mesons and baryons (see, e.g., Refs. [2,3]). In this respect the inclusion of QED effects in lattice QCD simulations has been carried out following mainly two methods: in the first one, QED is added directly to the action and QCD + QED simulations are performed at few values of the electric charge (see, e.g., Refs. [3,4]), while the second one, the RM123 approach of Refs. [2,5], consists in an expansion of the lattice path-

integral in powers of two small parameters [the e.m. coupling α_{em} and the light-quark mass difference $(m_d - m_u)/\Lambda_{\text{QCD}}$], which are both at the level of $\approx 1\%$. Since it suffices to work at leading order in the perturbative expansion, the attractive feature of the RM123 method is that the small values of the two expansion parameters are factorized out, so that one can get relatively large numerical signals for the slopes of the corrections with respect to the expansion parameters. Moreover, the slopes can be determined in isosymmetric QCD. In this Letter we adopt the RM123 method.

While the calculation of e.m. effects in the hadron spectrum does not suffer from infrared (IR) divergences, the same is not true in the case of hadronic amplitudes, where e.m. IR divergences are present and cancel for well-defined, measurable physical quantities only after including diagrams containing both real and virtual photons [6]. This is the case, for example, for the leptonic $\pi_{\ell 2}$ and $K_{\ell 2}$ and the semileptonic $K_{\ell 3}$ decays, which play a crucial role for an accurate determination of the Cabibbo-Kobayashi-Maskawa (CKM) entries $|V_{us}/V_{ud}|$ and $|V_{us}|$ [7].

The presence of IR divergences requires the development of additional strategies to those used in the computation of e.m. effects in the hadron spectrum. Such a new

Published by the American Physical Society under the terms of the [Creative Commons Attribution 4.0 International license](https://creativecommons.org/licenses/by/4.0/). Further distribution of this work must maintain attribution to the author(s) and the published article's title, journal citation, and DOI. Funded by SCOAP³.

strategy was proposed in Ref. [8], where the lattice determination of the decay rate of a charged pseudoscalar meson into either a final $\ell^\pm\nu_\ell$ pair or $\ell^\pm\nu_\ell\gamma$ state was addressed. Although it is possible in lattice simulations to compute the e.m. corrections due to the emission of real photons, this is not strictly necessary. Instead, the amplitude for the emission of a real photon can be computed in perturbation theory by limiting the maximum energy of the emitted photon in the meson rest frame, ΔE_γ , to be small enough so that the internal structure of the decaying meson is not resolved, but is larger than the experimental energy resolution [8]. The IR divergences are independent of the structure of the hadrons (i.e., they are universal) and cancel between diagrams containing a virtual photon (computed nonperturbatively) and those with the emission of a real photon (calculated perturbatively). In the intermediate steps of the calculation, however, it is necessary to introduce an IR regulator. We use the lattice volume L^3 itself as the IR regulator by working in the QED_L finite-volume formulation of QED [9] (for a recent review see [10]).

The inclusive rate $\Gamma(P_{\ell 2})$ can be expressed as [8]

$$\begin{aligned} \Gamma(P_{\ell 2}) &= \Gamma_0 + \Gamma_1^{\text{pt}}(\Delta E_\gamma) \\ &= \lim_{L \rightarrow \infty} [\Gamma_0(L) - \Gamma_0^{\text{pt}}(L)] \\ &\quad + \lim_{\mu_\gamma \rightarrow 0} [\Gamma_0^{\text{pt}}(\mu_\gamma) + \Gamma_1^{\text{pt}}(\Delta E_\gamma, \mu_\gamma)], \end{aligned} \quad (1)$$

where the subscripts 0, 1 indicate the number of photons in the final state and the superscript pt denotes the pointlike approximation for the decaying meson. The terms $\Gamma_0(L)$ and $\Gamma_0^{\text{pt}}(L)$ are evaluated on the lattice; both have the same IR divergences which, therefore, cancel in the difference. We use L as the intermediate IR regulator, and $\Gamma_0 - \Gamma_0^{\text{pt}}$ is independent of the regulator as this is removed [11]. Since all momentum modes contribute to it, $\Gamma_0(L)$ depends on the structure of P and must be computed nonperturbatively. In the second term on the rhs of Eq. (1), P is a pointlike meson and both $\Gamma_0^{\text{pt}}(\mu_\gamma)$ and $\Gamma_1^{\text{pt}}(\Delta E_\gamma, \mu_\gamma)$ can be calculated directly in infinite volume in perturbation theory, using a small photon mass μ_γ as the intermediate IR regulator. Each term is IR divergent, but the sum is convergent [6] and independent of the IR regulator. The explicit perturbative calculations of $\Gamma_0^{\text{pt}} + \Gamma_1^{\text{pt}}(\Delta E_\gamma)$ and $\Gamma_0^{\text{pt}}(L)$ have been performed in Refs. [8,11], respectively.

The inclusive decay rate (1) can be written as

$$\Gamma(P^\pm \rightarrow \ell^\pm\nu_\ell[\gamma]) = \Gamma_P^{(\text{tree})}(1 + \delta R_P), \quad (2)$$

where $\Gamma_P^{(\text{tree})}$ is the tree-level decay rate given by

$$\Gamma_P^{(\text{tree})} = \frac{G_F^2}{8\pi} |V_{q_1 q_2}|^2 m_\ell^2 \left(1 - \frac{m_\ell^2}{M_P^2}\right)^2 [f_P^{(0)}]^2 M_P, \quad (3)$$

where M_P is the physical mass of the charged P meson, including both e.m. and strong IB corrections. The

superscript (0) on a physical quantity denotes that it has been calculated in isosymmetric QCD (without QED). The P -meson decay constant, $f_P^{(0)}$ is defined by

$$A_P^{(0)} \equiv \langle 0 | \bar{q}_2 \gamma_0 \gamma_5 q_1 | P^{(0)} \rangle \equiv f_P^{(0)} M_P^{(0)}. \quad (4)$$

In Eq. (2) the quantity δR_P encodes the leading-order e.m. and strong IB corrections to the tree-level decay rate; its evaluation is described in Ref. [8]. Its value depends on the prescription used for the separation between the QED and QCD corrections, while the quantity $[f_P^{(0)}]^2(1 + \delta R_P)$ is prescription free. In this work we adopt the prescription in which the renormalized couplings and quark masses in the full theory and in isosymmetric QCD coincide in the $\overline{\text{MS}}$ scheme at a scale of 2 GeV [2,5] (see [12]).

In this Letter we focus on the ratio of the inclusive decay rates of kaons and pions into muons, namely,

$$\frac{\Gamma(K_{\mu 2})}{\Gamma(\pi_{\mu 2})} = \left| \frac{V_{us} f_K^{(0)}}{V_{ud} f_\pi^{(0)}} \right|^2 \frac{M_\pi^3}{M_K^3} \left(\frac{M_K^2 - m_\mu^2}{M_\pi^2 - m_\mu^2} \right)^2 (1 + \delta R_{K\pi}), \quad (5)$$

where $\delta R_{K\pi} \equiv \delta R_K - \delta R_\pi$. Using the gauge ensembles generated by the European Twisted Mass Collaboration (ETMC) with $N_f = 2 + 1 + 1$ light, strange, and charm sea quarks [13,14], we have calculated $\delta R_{K\pi}$, which, together with a lattice computation of $f_K^{(0)}/f_\pi^{(0)}$, allows us to determine $|V_{us}/V_{ud}|$ from the ratio in Eq. (5).

The quantity $\delta R_{K\pi}$ is less sensitive to various uncertainties than the individual terms δR_K and δR_π . Three main features help to reduce the systematic uncertainties in $\delta R_{K\pi}$. (i) In $\Gamma_0(L)$ all the terms up to $O(1/L)$ are ‘‘universal,’’ i.e., independent of the structure of the decaying hadron [11]. The residual, structure-dependent (SD) finite-volume effects (FVEs) start at order $O(1/L^2)$ and are found to be much milder in the case of $\delta R_{K\pi}$ (see the finite-volume section below). (ii) The matching of the bare lattice weak operator with the one renormalized using W regularization generates a mixing of operators of different chiralities when discretizations based on Wilson fermions, which break the chiral symmetry (such as twisted mass used here), are used. The mixing has been calculated only at order $O(\alpha_{em}\alpha_s)$ [8], but its effects cancel out in the difference $\delta R_{K\pi}$. (iii) Within SU(3) chiral perturbation theory (ChPT) the effects of the sea-quark electric charges depend on unknown low-energy constants starting at next-to-leading-order for δR_K and δR_π , but only at next-to-next-to-leading-order for $\delta R_{K\pi}$ [15]. Thus, the uncertainty due to the quenched QED (qQED) approximation, adopted in this Letter, is expected to be smaller for $\delta R_{K\pi}$.

Since the experimental rates $\Gamma(K_{\mu 2})$ and $\Gamma(\pi_{\mu 2})$ are inclusive, SD contributions to the real photon emission should be included. According to the ChPT predictions of Ref. [16], however, these contributions are negligible in the case of both kaon and pion decays into muons, while the

same does not hold as well in the case of final electrons (see Ref. [8]). This important finding will be investigated by an ongoing dedicated lattice study on the real photon emission amplitudes in light and heavy P -meson leptonic decays.

After extrapolating our lattice data to the physical pion mass and to the continuum and infinite volume limits, the main result of the present work is

$$\delta R_{K\pi}^{\text{phys}} = -0.0122 \pm 0.0016, \quad (6)$$

where the uncertainty includes both statistical and systematic errors, including an estimate of the uncertainty due to the QED quenching. Our result (6) can be compared with the current estimate $\delta R_{K\pi}^{\text{phys}} = -0.0112(21)$ from Refs. [17,18] adopted by the Particle Data Group (PDG) [19].

Details of the simulation.—The gauge ensembles used in this Letter were generated by the ETMC with $N_f = 2 + 1 + 1$ dynamical quarks and used in Ref. [20] to determine the up, down, strange, and charm quark masses. The main parameters of the simulations are collected in [12]. We employ the Iwasaki action [21] for gluons and the Wilson twisted mass action [22–24] for sea quarks. In the valence sector we adopt a nonunitary setup [25] in which the strange quark is regularized as an Osterwalder-Seiler fermion [26], while the up and down quarks have the same action as the sea. Working at maximal twist, such a setup guarantees an automatic $O(a)$ improvement [24,25]. The two valence quarks in the P meson are regularized with opposite values of the Wilson r parameter in order to guarantee that discretization effects on the P -meson mass are of order $\mathcal{O}(a^2\mu\Lambda_{\text{QCD}})$. The lepton ℓ is a free twisted-mass fermion with mass $m_\ell = m_\mu = 105.66$ MeV [19]. The neutrino is simply considered to be a free fermion field.

In this Letter we make use of the bootstrap samplings generated for the input parameters of the quark mass analysis of Ref. [20]. There, eight branches of the analysis were adopted differing in (i) the continuum extrapolation, adopting for the matching of the lattice scale either the Sommer parameter r_0 or the mass of a fictitious P meson made up of two valence strangelike (charmlike) quarks, (ii) the chiral extrapolation performed with fitting functions chosen to be either a polynomial expansion or a ChPT ansatz in the light-quark mass, and (iii) the choice between the methods $M1$ and $M2$, which differ by $O(a^2)$ effects, used to determine the mass renormalization constant $Z_m = 1/Z_P$ in the RI'-MOM scheme.

Evaluation of the amplitudes.—Following Ref. [8] the quantity $\delta R_K - \delta R_\pi$ is given by

$$\begin{aligned} \delta R_{K\pi} = & 2 \frac{\delta A_K}{A_K^{(0)}} - 2 \frac{\delta M_K}{M_K^{(0)}} + \delta\Gamma_K^{(\text{pt})}(\Delta E_\gamma) \\ & - 2 \frac{\delta A_\pi}{A_\pi^{(0)}} + 2 \frac{\delta M_\pi}{M_\pi^{(0)}} - \delta\Gamma_\pi^{(\text{pt})}(\Delta E_\gamma), \end{aligned} \quad (7)$$

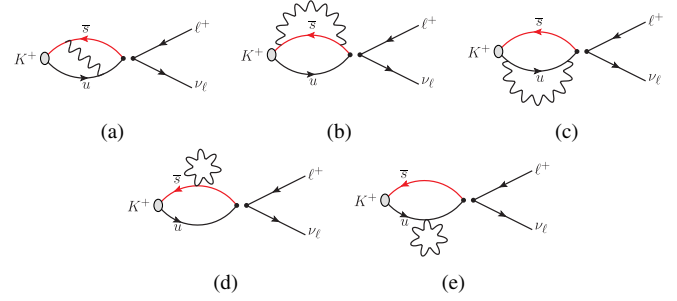


FIG. 1. Connected diagrams contributing at $O(\alpha_{em})$ to the $K^+ \rightarrow \ell^+ \nu_\ell$ decay amplitude, in which the photon is attached to quark lines: (a) exchange, (b),(c) self-energy, and (d),(e) tadpole diagrams.

where $\delta\Gamma_P^{(\text{pt})}(\Delta E_\gamma)$ represents the $O(\alpha_{em})$ correction to the tree-level decay rate for a pointlike meson and can be read off from Eq. (51) of Ref. [8], while δA_P and δM_P are the e.m. and IB corrections to the weak amplitude and mass of the P meson, respectively.

Within the qQED approximation, the evaluation of δA_P and δM_P requires the evaluation of only the connected diagrams shown in Figs. 1–4 for $K_{\ell 2}$ decays. The corrections δA_P and δM_P can be written as

$$\delta A_P = \delta A_P^{\text{QCD}} + \sum_{i=J,T,P,S} \delta A_P^i + \delta A_P^\ell, \quad (8)$$

$$\delta M_P = \delta M_P^{\text{QCD}} + \sum_{i=J,T,P,S} \delta M_P^i, \quad (9)$$

where δA_P^{QCD} (δM_P^{QCD}) represents the strong IB corrections corresponding to the diagrams of Fig. 3, while the other terms are QED corrections coming from the insertions of the e.m. current and tadpole operators of the pseudoscalar and scalar densities (see Refs. [2,27]).

In Eqs. (8) and (9), the term δA_P^ℓ (δM_P^ℓ) is generated by the diagrams of Figs. 1(a)–1(c), δA_P^T (δM_P^T) by the diagrams of Figs. 1(d)–1(e), δA_P^P (δM_P^P) by the diagrams of Figs. 2(a)–2(b), and δA_P^S (δM_P^S) by the diagrams of Figs. 3(a)–3(b). The term δA_P^ℓ corresponds to the photon exchange between the quarks and the final lepton. It arises from Figs. 4(a) and 4(b), while Fig. 4(c) (lepton wave function renormalization) can be safely omitted, since it cancels out exactly in the difference $\Gamma_0(L) - \Gamma_0^{\text{pt}}(L)$.

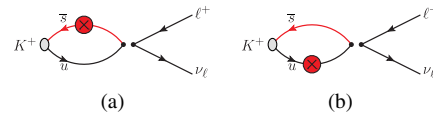


FIG. 2. Connected diagrams contributing at $O(\alpha_{em})$ to the $K^+ \rightarrow \ell^+ \nu_\ell$ decay amplitude corresponding to the insertion of the pseudoscalar density related to the e.m. shift of the critical mass, δm_f^{crit} , determined in Ref. [5].

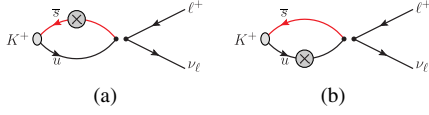


FIG. 3. Connected diagrams contributing at $O(\alpha_{em})$ and $O(m_d - m_u)$ to the $K^+ \rightarrow \ell^+ \nu_\ell$ decay amplitude related to the insertion of the scalar density (see Ref. [5]).

The evaluation of δM_P^{QCD} and the δM_P^i is described in Ref. [5], where the quark mass difference $(m_d - m_u)(\bar{M}\text{S}, 2 \text{ GeV}) = 2.38(18) \text{ MeV}$ was determined using the experimental charged and neutral kaon masses. The terms δA_P^{QCD} , δA_P^i , and δA_P^ℓ are extracted from the correlators described in Ref. [8]. Their numerical determination is illustrated briefly in Refs. [28,29] and in detail in Ref. [30]. The quality of the extraction of $\delta A_P^{\ell=\mu}/\delta A_P^{(0)}$ is illustrated in [12].

Finite-volume effects at $O(\alpha_{em})$.—The subtraction $\Gamma_0(L) - \Gamma_0^{\text{pt}}(L)$ makes the rate IR finite and cancels the structure-independent FVEs. The pointlike decay rate $\Gamma_0^{\text{pt}}(L)$ is given by

$$\Gamma_0^{\text{pt}}(L) = 2 \frac{\alpha_{em}}{4\pi} Y_P(L) \Gamma_P^{\text{tree}}, \quad (10)$$

where the factor $Y_P(L)$ is explicitly given by Eq. (98) of Ref. [11]. Equation (8) is therefore replaced by

$$\delta A_P = \delta A_P^{\text{QCD}} + \sum_i \delta A_P^i + \delta A_P^\ell - \frac{\alpha_{em}}{4\pi} Y_P(L) A_P^{(0)}, \quad (11)$$

where $Y_P(L)$ has the form

$$Y_P(L) = b_{\text{IR}} \log(M_P L) + b_0 + \frac{b_1}{M_P L} + \frac{b_2}{(M_P L)^2} + \frac{b_3}{(M_P L)^3} + O(e^{-M_P L}) \quad (12)$$

with the coefficients b_j ($j = \text{IR}, 0, 1, 2, 3$) depending on the dimensionless ratio m_ℓ/M_P [11]. The important point is that the SD FVEs start only at $O(1/L^2)$; i.e., all terms up to $O(1/L)$ in Eq. (12) are “universal” [11]. Being independent of the structure, they can be computed for a pointlike charged meson.

The FVE subtraction (11) up to order $O(1/L)$ is illustrated in Fig. 5 for δR_K , δR_π , and $\delta R_{K\pi}$ in the inclusive

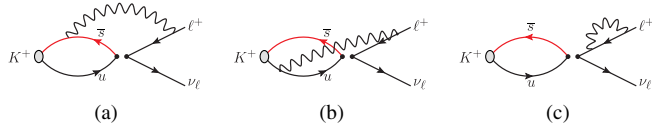


FIG. 4. Connected diagrams contributing at $O(\alpha_{em})$ to the $K^+ \rightarrow \ell^+ \nu_\ell$ decay amplitude corresponding to photon exchanges involving the final-state lepton.

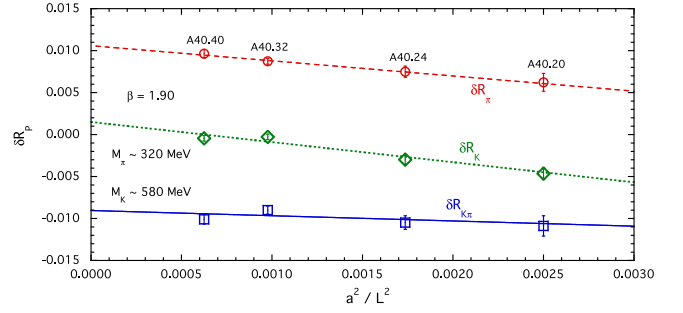


FIG. 5. Results for the corrections δR_π , δR_K , and $\delta R_{K\pi}$ for the gauge ensembles A40.20, A40.24, A40.32, and A40.40 sharing the same lattice spacing, pion and kaon masses, but different lattice sizes (see [12]). The universal FVEs, i.e., the terms up to order $O(1/L)$ in Eq. (12), are subtracted for each quantity. The lines are linear fits in $1/L^2$. The maximum photon energy ΔE_γ corresponds to the inclusive case $\Delta E_\gamma = \Delta E_\gamma^{\text{max},P} = M_P(1 - m_\mu^2/M_P^2)/2$.

case $\Delta E_\gamma = \Delta E_\gamma^{\text{max},P} = M_P(1 - m_\mu^2/M_P^2)/2$, which corresponds to $\Delta E_\gamma^{\text{max},K} \simeq 235 \text{ MeV}$ and $\Delta E_\gamma^{\text{max},\pi} \simeq 29 \text{ MeV}$, respectively. It can be seen that after subtraction of the universal terms the residual FVEs are almost linear in $1/L^2$ and ≈ 3 times smaller in the case of $\delta R_{K\pi}$.

Results for the ratio $\Gamma(K_{\ell 2})/\Gamma(\pi_{\ell 2})$.—The (inclusive) data for $\delta R_{K\pi}$, obtained using Eqs. (7), (11), and (12), are shown in Fig. 6. The “universal” FVEs are subtracted from the data and the combined chiral, continuum, and infinite-volume extrapolations are performed using the following ansatz:

$$\begin{aligned} \delta R_{K\pi} = & R_0 + R_\chi \log(m_{ud}) + R_1 m_{ud} + R_2 m_{ud}^2 + D a^2 \\ & + \frac{K_2}{L^2} \left(\frac{1}{M_K^2} - \frac{1}{M_\pi^2} \right) + \frac{K_2^\ell}{L^2} \left(\frac{1}{(E_\ell^K)^2} - \frac{1}{(E_\ell^\pi)^2} \right) \\ & + \delta \Gamma^{\text{pt}}(\Delta E_\gamma^{\text{max},K}) - \delta \Gamma^{\text{pt}}(\Delta E_\gamma^{\text{max},\pi}), \end{aligned} \quad (13)$$

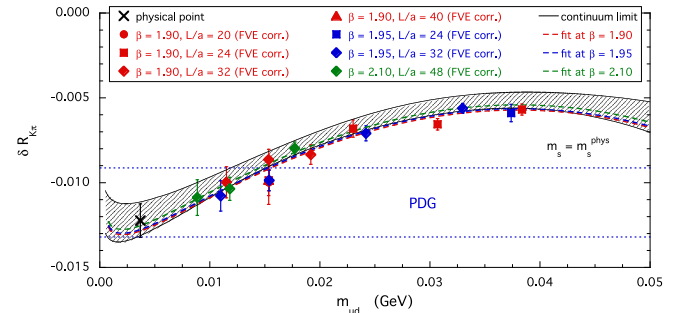


FIG. 6. Results for the correction $\delta R_{K\pi}$ [Eqs. (7) and (11)] after the subtraction of both the universal FVEs in Eq. (12) and the residual FVEs obtained from the fitting function (13). The dashed lines are the (central) results at each β , while the shaded area identifies the continuum limit at the $1\text{-}\sigma$ level. The cross is the extrapolated value at $m_{ud}^{\text{phys}}(\bar{M}\text{S}, 2 \text{ GeV}) = 3.70(17) \text{ MeV}$ [20]. The blue dotted lines correspond to the value $-0.0112(21)$ from Refs. [17,18] adopted by the PDG [19]. Errors are statistical only.

where m_{ud} is the renormalized u/d quark mass, $E_\ell^P = M_P(1 + m_\ell^2/M_P^2)/2$ is the lepton energy in the P -meson rest frame, and $R_{0,1,2}$, D , K_2 , and K_2^ℓ are free parameters. In Eq. (13) the chiral coefficient R_χ is known [15] and given by $R_\chi = \alpha_{em}(2Z/9 - 3)/4\pi$ in qQED, where Z is obtained from the chiral limit of the $O(\alpha_{em})$ correction to $M_{\pi^\pm}^2$ [i.e., $\delta M_{\pi^\pm}^2 = 4\pi\alpha_{em}Zf_0^2 + O(m_{ud})$]. In Ref. [5] we found $Z = 0.658(40)$.

Using Eq. (13) we have fitted the data for $\delta R_{K\pi}$ using a χ^2 -minimization procedure with an uncorrelated χ^2 , obtaining values of $\chi^2/\text{d.o.f.}$ always around 1.2. The uncertainties on the fitting parameters do not depend on the χ^2 value, because they are obtained using the bootstrap samplings of Ref. [20] (see the section on simulations, above). This guarantees that all the correlations among the data points and among the fitting parameters are properly taken into account. The quality of our fits is illustrated in Fig. 6.

At the physical pion mass in the continuum and infinite-volume limits we obtain

$$\begin{aligned} \delta R_{K\pi}^{\text{phys}} &= -0.0122(10)_{\text{stat}}(2)_{\text{input}}(8)_{\text{chir}}(5)_{\text{FVE}}(4)_{\text{disc}}(6)_{\text{qQED}} \\ &= -0.0122(16), \end{aligned} \quad (14)$$

where $(\)_{\text{stat}}$ indicates the uncertainty induced by both the statistical errors and the fitting procedure itself, $(\)_{\text{input}}$ is the error coming from the uncertainties of the input parameters of the quark-mass analysis of Ref. [20], $(\)_{\text{chir}}$ is the difference between including or excluding the chiral logarithm in the fits (i.e., taking $R_\chi \neq 0$ or $R_\chi = 0$), $(\)_{\text{FVE}}$ is the difference between including ($K_2 \neq 0$ and $K_2^\ell \neq 0$) or excluding ($K_2 = K_2^\ell = 0$) the residual FVE correction in $\delta R_{K\pi}$ [30], $(\)_{\text{disc}}$ is the uncertainty coming from including ($D \neq 0$) or excluding ($D = 0$) the discretization term proportional to a^2 , and $(\)_{\text{qQED}}$ is our estimate of the uncertainty of the QED quenching. This is obtained using the ansatz (13) with the coefficient R_χ of the chiral log fixed at the value $R_\chi = \alpha_{em}(Z - 3)/4\pi$, which includes the effects of the up, down, and strange sea-quark charges [15]. The change in $\delta R_{K\pi}^{\text{phys}}$ is $\simeq 0.003$, which has been already added in the central value of Eq. (14). To be conservative, we use twice that value for our estimate of the qQED uncertainty.

Our result (14) can be compared to the value $\delta R_{K\pi}^{\text{phys}} = -0.0112(21)$ from Refs. [17,18] adopted by the PDG [19]. Using in Eq. (5) the experimental $K_{\mu 2}$ and $\pi_{\mu 2}$ decay rates [19], we obtain

$$\left| \frac{V_{us}}{V_{ud}} \frac{f_K^{(0)}}{f_\pi^{(0)}} \right| = 0.27673(29)_{\text{exp}}(23)_{\text{th}}, \quad (15)$$

where the first error comes from experiments and the second one is related to the uncertainty in our result (14).

Adopting the $N_f = 2 + 1 + 1$ Flavour Lattice Averaging Group average $f_K^{(0)}/f_\pi^{(0)} = 1.1958(26)$ [1] (see [12]), one gets

$$\left| \frac{V_{us}}{V_{ud}} \right| = 0.23142(24)_{\text{exp}}(54)_{\text{th}}. \quad (16)$$

Using the value $|V_{ud}| = 0.97417(21)$ from superallowed nuclear beta decays [31], one then has

$$|V_{us}| = 0.22544(58). \quad (17)$$

Thus, using $|V_{ub}| = 0.00413(49)$ [19] the first-row CKM unitarity is confirmed to be below the per mille level, viz.,

$$|V_{ud}|^2 + |V_{us}|^2 + |V_{ub}|^2 = 0.99985(49). \quad (18)$$

We gratefully acknowledge the CPU time provided by PRACE under Project No. Pra10-2693 and by CINECA under the initiative INFN-LQCD123 on the BG/Q system. Fermi, V. L., G. M., S. S., and C. T. thank MIUR (Italy) for partial support under Contract No. PRIN 2015P5SBHT. G. M. also acknowledges partial support from ERC Ideas Advanced Grant No. 267985 ‘‘DaMeSyFla.’’ C. T. S. was partially supported by STFC (UK) Grants No. ST/L000296/1 and No. ST/P000711/1.

-
- [1] S. Aoki *et al.*, *Eur. Phys. J. C* **77**, 112 (2017).
 [2] G. M. de Divitiis, R. Frezzotti, V. Lubicz, G. Martinelli, R. Petronzio, G. C. Rossi, F. Sanfilippo, S. Simula, and N. Tantalo (RM123 Collaboration), *Phys. Rev. D* **87**, 114505 (2013).
 [3] S. Borsanyi *et al.*, *Science* **347**, 1452 (2015).
 [4] P. Boyle, V. Gülpers, J. Harrison, A. Jüttner, C. Lehner, A. Portelli, and C. T. Sachrajda, *J. High Energy Phys.* **09** (2017) 153.
 [5] D. Giusti, V. Lubicz, C. Tarantino, G. Martinelli, F. Sanfilippo, S. Simula, and N. Tantalo (RM123 Collaboration), *Phys. Rev. D* **95**, 114504 (2017).
 [6] F. Bloch and A. Nordsieck, *Phys. Rev.* **52**, 54 (1937).
 [7] N. Cabibbo, *Phys. Rev. Lett.* **10**, 531 (1963); M. Kobayashi and T. Maskawa, *Prog. Theor. Phys.* **49**, 652 (1973).
 [8] N. Carrasco, V. Lubicz, G. Martinelli, C. T. Sachrajda, N. Tantalo, C. Tarantino, and M. Testa, *Phys. Rev. D* **91**, 074506 (2015).
 [9] M. Hayakawa and S. Uno, *Prog. Theor. Phys.* **120**, 413 (2008).
 [10] A. Patella, *Proc. Sci.*, LATTICE2016 (2017) 020 [arXiv:1702.03857].
 [11] V. Lubicz, G. Martinelli, C. T. Sachrajda, F. Sanfilippo, S. Simula, and N. Tantalo, *Phys. Rev. D* **95**, 034504 (2017).
 [12] See the Supplemental Material at <http://link.aps.org/supplemental/10.1103/PhysRevLett.120.072001> for the discussion of the main parameters of the isosymmetric QCD

- simulations and for the sketch of some of the key points of the numerical analysis.
- [13] R. Baron *et al.* (ETM Collaboration), *J. High Energy Phys.* **06** (2010) 111.
- [14] R. Baron *et al.* (ETM Collaboration), *Proc. Sci.*, LATTICE2010 (2010) 123 [[arXiv:1101.0518](#)].
- [15] J. Bijnens and N. Danielsson, *Phys. Rev. D* **75**, 014505 (2007).
- [16] V. Cirigliano and I. Rosell, *J. High Energy Phys.* **10** (2007) 005.
- [17] J. L. Rosner *et al.*, [arXiv:1509.02220](#).
- [18] V. Cirigliano and H. Neufeld, *Phys. Lett. B* **700**, 7 (2011).
- [19] C. Patrignani *et al.* (Particle Data Group), *Chin. Phys. C* **40**, 100001 (2016).
- [20] N. Carrasco *et al.* (ETM Collaboration), *Nucl. Phys.* **B887**, 19 (2014).
- [21] Y. Iwasaki, *Nucl. Phys.* **B258**, 141 (1985).
- [22] R. Frezzotti *et al.* (Alpha Collaboration), *J. High Energy Phys.* **08** (2001) 058.
- [23] R. Frezzotti and G. C. Rossi, *Nucl. Phys. B, Proc. Suppl.* **128**, 193 (2004).
- [24] R. Frezzotti and G. C. Rossi, *J. High Energy Phys.* **08** (2004) 007.
- [25] R. Frezzotti and G. C. Rossi, *J. High Energy Phys.* **10** (2004) 070.
- [26] K. Osterwalder and E. Seiler, *Ann. Phys. (N.Y.)* **110**, 440 (1978).
- [27] G. M. de Divitiis *et al.*, *J. High Energy Phys.* **04** (2012) 124.
- [28] V. Lubicz *et al.*, *Proc. Sci.*, LATTICE2016 (2016) 290 [[arXiv:1610.09668](#)].
- [29] S. Simula, *Proc. Sci.*, CKM2016 (2017) 032 [[arXiv:1704.00510](#)].
- [30] D. Giusti *et al.* (to be published).
- [31] J. C. Hardy and I. S. Towner, *Phys. Rev. C* **91**, 025501 (2015).